

# Perturbation-mitigated USV Navigation with Distributionally Robust Reinforcement Learning

Zhaofan Zhang<sup>1</sup>, Minghao Yang<sup>1</sup>, Sihong Xie<sup>1\*</sup>, Hui Xiong<sup>1,2\*</sup>

<sup>1</sup>The Hong Kong University of Science and Technology (Guangzhou)

<sup>2</sup>The Hong Kong University of Science and Technology

## Abstract

The robustness of Unmanned Surface Vehicles (USV) is crucial when facing unknown and complex marine environments, especially when heteroscedastic observational noise poses significant challenges to sensor-based navigation tasks. Recently, Distributional Reinforcement Learning (DistRL) has shown promising results in some challenging autonomous navigation tasks without prior environmental information. However, these methods overlook situations where noise patterns vary across different environmental conditions, hindering safe navigation and disrupting the learning of value functions. To address the problem, we propose DRIQN to integrate Distributionally Robust Optimization (DRO) with implicit quantile networks to optimize worst-case performance under natural environmental conditions. Leveraging explicit subgroup modeling in the replay buffer, DRIQN incorporates heterogeneous noise sources and target robustness-critical scenarios. Experimental results based on the risk-sensitive environment demonstrate that DRIQN significantly outperforms state-of-the-art methods, achieving +13.51% success rate, -12.28% collision rate and +35.46% for time saving, +27.99% for energy saving, compared with the runner-up.

## Introduction

Autonomous navigation is the keystone capability that transforms an USV from a remotely operated craft into a truly independent maritime agent. Reliable navigation empowers USVs to undertake long-duration missions ranging from port oil spill cleanup (Elmakis and Degani 2023) and environmental monitoring (Tran et al. 2024) to border security (Fernandes et al. 2025) and search-and-rescue (Wang et al. 2023b) while simultaneously reducing operational risk, human exposure, and overall cost. In these maritime navigation tasks, the environment is characterized by complexity and partial observability. The intricate variations in water currents are difficult to monitor in real-time, and obstacles such as reefs may also be encountered (Lolla, Haley Jr, and Lermusiaux 2015). Moreover, the perception devices used by the robot may face various unobservable interferences within the environment, resulting in noisy observations (Vieira et al. 2020). Specifically, heterogeneous extreme natural conditions (e.g., weather, sea state, geographic

\*Corresponding authors.  
Preprint.

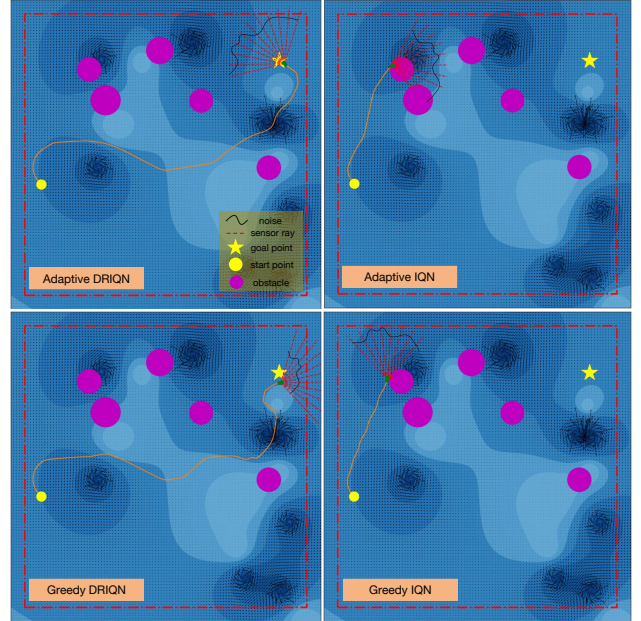


Figure 1: **Proposed DRIQN vs. IQN:** Policy trajectories visualization with observational noise from sensor. For IQN-based methods, we investigate adaptive strategy and greedy strategy with details in Section *Metrics and Strategy*.

locality) induce trajectory-specific, non-stationary observational noise. For instance, as illustrated in Figure 1, the observational perturbation exacerbates the inherent uncertainty of complex marine environments and impedes accurate risk-sensitive policy learning based on corrupted observation, creating substantial navigation hazards for USVs.

Prior works on USV navigation can be mainly grouped into: (i) *model-based* methods (Wang et al. 2023a; Menges, Tengesdal, and Rasheed 2024; Asfihani, Maulana Syafi'i, and Hasan 2025); (ii) models with *prior-dependent* knowledge (Han et al. 2016; Hong et al. 2024); (iii) *direct observation-driven decision-making* approaches (e.g., APF (Sun et al. 2019), BA (McGuire, de Croon, and Tuyls 2018) and reinforcement learning (Wang et al. 2022; Lin, McConnell, and Englot 2023)). Direct observation-driven approaches make decisions based on sensor observation with-

out prior environmental knowledge and extra modeling design. Despite promising results, model-based approaches (e.g., nonlinear MPC) incorporate analytical vehicle dynamics into optimal control, requiring high-fidelity models and suffering degradation under uncertainties. Prior-dependent methods further face limitations in prior availability and freshness, incurring substantial precomputation overhead. In contrast, observation-driven decision-making methods offer a generalizable, prior-independent solution for navigation in unknown environments, albeit with heightened sensitivity to observational noise. Recently, as one kind of prominent observation-driven decision-making method, Deep Reinforcement Learning (DRL) has emerged for robotic navigation in complex environments (Lee, Kim, and Choi 2023; Hossain et al. 2024). Building on this advantage, some DistRL methods (Lin, McConnell, and Englot 2023; Liu, van Kampen, and De Croon 2023) enable risk-sensitive navigation through quantile-based return distribution modeling. By employing task-specific reward designs and distortion functions with Conditional Value-at-Risk (CVaR), DistRL reshapes return distributions to focus on critical lower-tail outcomes while constraining distributional support, thereby enhancing robust policy learning. Nevertheless, without environmental priors or modeling knowledge for constraint factors, these approaches cannot be readily optimized via constructing robust mechanisms, thereby lacking explicit safety guarantees under heterogeneous noise-corrupted observations. This presents a pressing research challenge: how can we ensure the safety of unmanned surface navigation in multi-noise-corrupted marine environment just using a data-driven optimization approach?

To address the challenge, we propose Distributionally Robust Implicit Quantile Networks (DRIQN), a novel framework ensuring risk-sensitive policies via quantile regression under observational noise. Leveraging distributionally robust optimization, DRIQN reformulates the DRO problem as a semi-definite program (Eq. 13) to holistically address diverse noise influences. Crucially, DRIQN implements “gradient substitution” replacing the network’s output-layer gradients with DRO-based gradients to enhance robustness without auxiliary modules. Considering the scalability challenge of DRO caused by the large-scale datapoint-level optimization process, we transform standard datapoint-based DRO by leveraging transition data’s inherent structure: under specific environmental conditions, noisy transitions naturally form homogeneous subgroups following corresponding noise patterns. This structural property enables reformulating the original datapoint-level DRO problem as the supremum over subgroup-level loss functions. Each subgroup represents unlabeled transition data clusters with distinct noise characteristics. Experimental results demonstrate that DRIQN significantly outperforms baselines: achieving +13.51% success rate, -12.28% collision rate and +35.46% for time saving, +27.99% for energy saving, compared with the runner-up. To our knowledge, DRIQN is the first method tackling multiple observational noise patterns from natural conditions, enabling robust risk-sensitive policies for USV navigation.

The main contributions of this paper are as follows:

- We propose a novel, streamlined distributionally robust optimization framework that enhances RL agent performance against perturbed observations through substitution of DRO-based gradients.
- We present a risk-sensitive and robust navigation approach for developing an online path planner by unifying DistRL and DRO, maintaining robustness and safety in the presence of complex environmental noise patterns.
- Simulated experiments show the resulted planner enabled the vehicle to resist the impact of observational perturbation and reach the goal as safely as possible under strong disturbances, unknown flows and obstacles.

## Related Work

Among three paradigms (model-based, prior-dependent, and direct observation-driven decision-making) in USV navigation, observation-driven methods offer enhanced generality and reduced prior knowledge requirements for path planning in unknown environments. As a foundational observation-driven navigation approach, Artificial Potential Field (APF) methods (Khatib 1985; Sun et al. 2019) navigate robots via goal-attractive and obstacle-repulsive forces, yet suffer from local minima and goal-proximity failures. Separately, Bug Algorithms (Lumelsky and Stepanov 1986) and recent variants Bug1/Bug2 (McGuire, de Croon, and Tuyls 2018) utilize boundary-following for reactive planning but generate highly suboptimal paths due to exhaustive obstacle perimeter traversal. Recently, DRL has been widely applied in navigation tasks. Considering safety in navigation task, safe RL methods (Lütjens, Everett, and How 2018; Dawood, Shokry, and Bennewitz 2024; Tomilin, Fang, and Pechenizkiy 2025) enforce navigation safety via constrained optimization, yet require handcrafted constraints and remain vulnerable to catastrophic failures during transient violations. DistRL’s efficiency-safety balance promotes adoption in risk-sensitive applications (e.g., quadruped locomotion (Shi et al. 2024a), pursuit-evasion (Zhang, Zhao, and Ren 2025), USV/UAV navigation (Lin, McConnell, and Englot 2023; Liu, van Kampen, and De Croon 2023)). However, severe noise induces sharp performance decay, compromising both success rates and safety in noisy missions.

Considering robustness, distributionally robust optimization is an effective approach for data-driven decision-making in the presence of uncertainty (Nietert, Goldfeld, and Shafiee 2023). The DRO problem is a minimax optimization that seeks a decision minimizing the worst-case expected loss within a distributional uncertainty set. By defining the uncertainty set based on the empirical data distribution, DRO method learns a model that remains robust to distributional uncertainties of data (Staib and Jegelka 2019). Whereas expected-value optimization under domain randomization (Tobin et al. 2017) does not directly control worst-case degradation, a DRO formulation emphasizes adverse extremes, thereby aligning with navigation safety. Several studies employ DRO to enhance model robustness. However, these methods exhibit limitations: some necessitate auxiliary components (e.g., generative models (Shi et al. 2024b; Ramesh et al. 2024)) that complicate deployment;

others are model-based (Shi and Chi 2024; He et al. 2025) or rely on offline data (Leung et al. 2025). Such drawbacks restrict their applicability in real-world settings where RL agents must interact with environments online without prior environmental information and modeling design.

## Problem Formulation

An USV does not have full knowledge of the environment, but instead receives noisy partial observations of robot’s surroundings constrained by the limited sensing range of its sensors. We formulate the USV navigation problem as a *perturbed* Partially Observable Markov Decision Process  $\mathcal{M}$ , denoted as  $(\mathcal{S}, \mathcal{A}, \mathcal{O}, \mathcal{P}, R, \gamma, \nu)$ , where  $\mathcal{S}$ ,  $\mathcal{A}$  and  $\mathcal{O}$  represent the state, action and observation space, respectively. At each time step  $t$ , the agent receives a corrupted observation  $\nu(o_t)$  subject to natural disturbances, where  $o_t \in \mathcal{O}$  denotes the observation of current state  $s_t$ . Based on this observation, the agent selects an action  $a_t \in \mathcal{A}$  according to policy  $\tilde{\pi}(a_t \mid \nu(o_t))$ . This leads the agent to transition to the next state  $s_{t+1} \sim \mathcal{P}(\cdot \mid s_t, a_t)$ , and the agent receives a reward  $r_t \sim R(s_t, a_t)$ , as well as a perturbed observation  $\nu(o_{t+1})$  of  $s_{t+1}$ . Following observation-disturbed policy  $\tilde{\pi}$ , the discounted sum of future rewards is represented as the random variable  $Z^{\tilde{\pi}}(s_t, a_t)$ , defined as  $Z^{\tilde{\pi}}(s_t, a_t) = \sum_{k=0}^{\infty} \gamma^k R(s_{t+k}, a_{t+k})$ , where  $\gamma \in (0, 1)$  denotes the discount factors and determines the relative importance of future rewards. The objective of standard RL under noisy observations is to maximize the expected discounted return, formalized by the value function:  $Q^{\tilde{\pi}}(s_t, a_t) = \mathbb{E}[Z^{\tilde{\pi}}(s_t, a_t)]$ . Expectations are risk-neutral, representing returns solely through  $Q^{\tilde{\pi}}(s, a)$ . DistRL addresses the limited expressiveness of this expectation by estimating the distribution of  $Z^{\tilde{\pi}}(s, a)$ . Environmental noise incorporated into the state transition kernel augments the state representation. This formulation preserves the Bellman operator’s monotonicity and  $\gamma$ -shift invariance, enabling value function evaluation for any stationary policy.

## Methodology

In this section, we elaborate on our DRO-enhanced DistRL method, DRIQN. We start by revisiting the theoretical foundations of DistRL, then formalize the task environment, and finally elucidate the architecture of the DRIQN approach.

### Distributional Reinforcement Learning

Distributional Reinforcement Learning explicitly models the return distribution  $Z$  governed by the following *distributional* Bellman equation and optimality equation:

$$Z^{\pi}(s, a) \stackrel{D}{=} R(s, a) + \gamma Z^{\pi}(s', a'), \quad (1)$$

$$\mathcal{T}Z^{\pi}(s, a) \stackrel{D}{=} R(s, a) + \gamma Z^{\pi}\left(s', \arg\max_{a'} \mathbb{E}[Z^{\pi}(s', a')]\right), \quad (2)$$

where  $\stackrel{D}{=}$  indicates equality in distribution, and  $\mathcal{T}$  represents the *distributional Bellman optimality operator*.

We utilize DistRL with IQN as a risk-sensitive path planner that has achieved promising performance in many tasks

of robotics (Liu, van Kampen, and De Croon 2023; Lin, McConnell, and Englot 2023; Shi et al. 2024a). IQN utilizes the quantiles to provide a flexible representation of return distribution  $Z$ , denoted as  $Z_{\tau} := F_Z^{-1}(\tau)$ , where  $\tau \sim U([0, 1])$  and  $F^{-1}$  is inverse cumulative distribution function. To effectively capture risk-sensitive behaviors, IQN incorporates a distortion function  $\beta$  to adjust the quantile distribution, emphasizing certain regions of the return distribution. Then the distorted expectation of  $Z$  under  $\beta : [0, 1] \rightarrow [0, 1]$  is defined by:

$$Q_{\beta}(s, a) = \mathbb{E}_{\tau \sim U([0, 1])}[Z_{\beta(\tau)}(s, a)]. \quad (3)$$

The standard deep  $Q$ -Learning framework trains a neural network-based state-action value function by iteratively minimizing a loss function, which is defined through the temporal difference (TD) error. The TD error is defined as:

$$\delta = r + \gamma \max_{a'} Q(s', a') - Q(s, a). \quad (4)$$

The IQN loss function integrates the sampled temporal difference error (Eq. (6)) with the *Huber* quantile regression (Huber 1992) (Eq. (7)) to optimize the quantile value network:

$$\mathcal{L}_{IQN}(s, a, r, s') = \frac{1}{N'} \sum_{i=1}^N \sum_{j=1}^{N'} \rho_{\tau_i}^{\kappa}(\delta^{\tau_i, \tau'_j}) \quad (5)$$

where  $N$  and  $N'$  denote the counts of i.i.d. samples  $\{\tau_i\}_{i=1}^N$  and  $\{\tau'_j\}_{j=1}^{N'}$  from  $\mathcal{U}([0, 1])$ . The temporal difference error and Huber loss components are:

$$\delta^{\tau_i, \tau'_j} = r + \gamma Z_{\tau'_j}(s', a') - Z_{\tau_i}(s, a) \quad (6)$$

$$\rho_{\tau}^{\kappa}(u) = |\tau - \mathbb{I}_{\{u < 0\}}| \left( \frac{\mathcal{L}_{\kappa}(u)}{\kappa} \right) \quad (7)$$

$$\mathcal{L}_{\kappa}(u) = \begin{cases} \frac{1}{2}u^2, & |u| \leq \kappa \\ \kappa(|u| - \kappa/2), & \text{otherwise} \end{cases}$$

This integrated loss formulation ensures convex optimization of quantile representations during gradient-based training. The corresponding policy approximation uses  $K$  quantile samples  $\tilde{\tau}_k \sim \mathcal{U}([0, 1])$ :

$$\tilde{\pi}_{\beta}(s) = \arg\max_a \frac{1}{K} \sum_{k=1}^K Z_{\beta(\tilde{\tau}_k)}(s, a) \quad (8)$$

with actions selected through  $\tilde{\pi}_{\beta}(s)$ .

### USV Navigation under Observational Perturbation

In this task, the vehicle must reach the goal while handling natural observation noise, avoiding obstacles, and adapting to flow disturbances. The key components of RL are designed as follows:

**Reward.** To learn a policy that moves toward the goal while avoiding obstacles, the reward function is designed as:  $r_t = r_{\text{step}} + \alpha(d_{t-1} - d_t) + r_{\text{collision}}\mathbb{I}_{\text{collision}} + r_{\text{goal}}\mathbb{I}_{\text{goal}}$ , where  $d_t$  represents the distance between the robot and the goal at time  $t$ . The indicator function  $\mathbb{I}_{\text{collision}}$  (resp.  $\mathbb{I}_{\text{goal}}$ ) takes the value of 1 if collision happens (the goal is reached, resp)

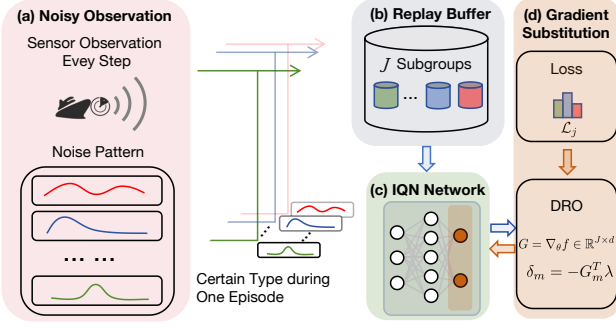


Figure 2: **Overall framework of our method.** In (a), the USV receives noisy observations specific to its current natural condition, assuming a consistent noise pattern within one episode due to proximity of environmental condition. Therefore, the replay buffer in (b) accumulates subgroups with distinct noise patterns. This variation has a significant impact on the training of the implicit quantile networks in (c). To enhance robustness, DRIQN employs “Gradient Substitution” in (d), replacing the gradients of the output layer with those computed via DRO.

at  $t$ , and 0 otherwise. The components of reward are set as  $r_{\text{step}} = -1.0$ ,  $r_{\text{collision}} = -50.0$ ,  $r_{\text{goal}} = 100.0$ , and  $\alpha = 1.0$ .

**Observation.** Based on real-world device, the observation at time step  $t$  is given by:  $O_t = (O_{\text{velocity}}, O_{\text{goal}}, O_{\text{LiDAR}})$ , where  $O_{\text{velocity}}$  denotes the robot’s seafloor-relative velocity.  $O_{\text{goal}}$  represents the goal position in the robot’s frame.  $O_{\text{LiDAR}}$  consists of LiDAR reflections, which provide information about detected obstacles.

**Action.** The robot’s action at time step  $t$  is defined as:  $a_t = (a(t), w(t))$ , where  $a(t)$  represents the rate of change in velocity magnitude, and  $w(t)$  denotes the rate of change in velocity direction. The available action space is:  $a \in \{-0.4, 0.0, 0.4\} \text{ m/s}^2$ ,  $w \in \{-0.52, 0.0, 0.52\} \text{ rad/s}$ . The forward speed is constrained within  $[0, v_{\text{max}}]$ .

**Observational Perturbation.** Since our objective is to model natural noise shaped by coupled climate, meteorological, illumination, and sea-state effects instead of adversarial attack scene, we rely on broadly observed, non-synthetic noise sources with specifications given in Section *Experimental Settings*.

## Distributionally Robust Optimization for DistRL

IQN has demonstrated superior performance as a risk-sensitive policy for path planning in an ideal environment. However, the planner relies on online distributional reinforcement learning training without prior information, meaning that errors in actions under noisy observations will cause reward signal mismatching and policy deviation. This issue is exacerbated by the presence of multiple noise subgroups within the replay buffer. Despite its impact, this problem remains largely unexplored in existing research.

We first reformulate the algorithm’s robustness facing noisy transition data as an optimization problem and then apply DRO to handle different patterns of noise that perceptions of robot sensors have. The framework of DRIQN is

shown in Figure 2.

Based on previous optimization works about DRO (Qi et al. 2020; Shen et al. 2022), the form of optimization target can be written as:

$$\min_{\theta \in \mathbb{R}^d} F_p(\theta) = \min_{\theta \in \mathbb{R}^d} \sup_{\mathbf{P} \in \mathbb{R}^n} \sum_{i=1}^n p_i \mathcal{L}_{IQN}(T_i) - d(\mathbf{P}, \mathbf{1}/n), \quad (9)$$

where  $\mathcal{L}_{IQN}$  denotes the IQN loss function applied to the noisy transition datapoint  $T_i = (s_i, a_i, r_i, s_{i+1})$  from replay buffer of size  $n$ . The IQN model uses parameters  $\theta \in \mathbb{R}^d$ , while  $\mathbf{P} = (p_1, \dots, p_n)$  denotes noise-characterizing density ratios satisfying  $\sum p_i = 1$  and  $p_i > 0$ .  $d(\mathbf{P}, \mathbf{1}/n)$  quantifies the difference between  $\mathbf{P}$  and the uniform probabilities  $\mathbf{1}/n$ .

To adapt the DRO to big data and large parameter scenario, we focus on the uncertainty set  $\mathcal{Q}$ , which is partitioned into  $J$  subgroups that represent the subgroups of transition data with different noise types. Based on this replay buffer partition, we propose an efficient gradient-based learning approach to solve the optimization problem.

Given identical noise types per subgroup, we implement independent data sampling across all replay buffer subgroups. To further improve both comprehensive robustness and data utilization efficiency beyond the worst-case subgroup, we propose computing the optimization gradient as a linear combination of the gradients from noisy subgroups. The optimization gradient in DRIQN is used to replace the original gradient during the backpropagation through the last quantiles layer of the IQN network.

We formalize the inner term of DRO problem Eq. (9) with a partitioned uncertainty set  $\mathcal{Q}$ . For simplicity, we construct  $\mathcal{Q}$  through considering limited  $J$  kinds of noise, i.e.  $\mathcal{Q} := \{q_1, q_2, \dots, q_J\}$ .

$$\sup_{\mathbf{P} \in \mathbb{R}^J, q \in \mathcal{Q}} \sum_{j=1}^J p_j \mathbb{E}_{(T_j) \sim q_j} [\mathcal{L}_{IQN}(T_j)] - d(\mathbf{P}, \mathbf{1}/J). \quad (10)$$

To ensure a fair comparison of natural-condition-induced noise types, we assume equiprobable occurrence for all categories. Formally, we define  $\mathbf{P}$  as a uniform probability vector, which yields  $d(\mathbf{P}, \mathbf{1}/J) = 0$  in the final term. So the inner term of DRO will be expressed as:

$$\sup_{q \in \mathcal{Q}} \mathbb{E}_{T \sim q} [\mathcal{L}_{IQN_q}(T)]. \quad (11)$$

Now we go back to the complete DRO minimax term Eq. (9). To solve the problem, we aim to minimize the expected loss over the uncertainty set  $\mathcal{Q}$  following:

$$\min_{\theta} \max_{1 \leq j \leq J} \frac{1}{c_j} \sum_{k=1}^{c_j} \mathcal{L}_{IQN}(T_{jk}), \quad (12)$$

where  $J$  is the number of noise subgroups,  $c_j$  is the number of samples in subgroup  $j$  that has unique noise type,  $T_{jk}$  refers to the  $k$ -th transition data in the  $j$ -th subgroup. Our method provides a more scalable and efficient way to obtain the gradient descent direction by solving optimization problem Eq. (12) through learning the supremum of the set of loss functions with respect to each noise subgroup.

As the optimization problem described in Eq. (12), the right side noted as  $f_j(\theta) = \frac{1}{c_j} \sum_{k=1}^{c_j} \mathcal{L}_{IQN}(T_{jk})$  during the iteration  $m$  can be linearized to achieve convex approximation, therefore we rewrite the right side as  $f_j(\theta_m) + \langle \nabla f_j(\theta_m), \theta - \theta_m \rangle$ .

Since the inner term for max operation has been smoothed by linearization, to ensure finding the stable descent direction during the min stage when  $\max_{1 \leq j \leq J} f_j(\theta_m) + \langle \nabla f_j(\theta_m), \theta - \theta_m \rangle$  is not strictly convex with respect to parameter  $\theta$ . Thus, we add a regularization term  $\|\theta - \theta_m\|_2$ . The gradient descent direction is set as  $\delta := \theta - \theta_m$ , we obtain the equivalent form of the DRO problem:

$$\min_{\delta, \kappa} \|\delta\|_2 + \kappa, \quad (13a)$$

$$\text{s.t. } f_j(\theta_m) + \langle \nabla f_j(\theta_m), \delta \rangle \leq \kappa, \forall 1 \leq j \leq J. \quad (13b)$$

**Theorem 1** (Equivalent dual quadratic program). *Let  $\theta_m \in \mathbb{R}^d$  be the model parameter at iteration  $m$  and define the subgroup losses  $f_j(\theta)$ ,  $j = 1, \dots, J$ . Denote  $G_m := \nabla_\theta f(\theta_m) \in \mathbb{R}^{J \times d}$ , whose  $j$ -th row is  $\nabla_\theta f_j(\theta_m)^\top$ , and consider the quadratic program in Eq. (13). The unique optimal descent direction of this problem is a convex combination form:*

$$\delta_m^* = -G_m^\top \lambda^*, \quad \lambda^* \in \Delta_J := \left\{ \lambda \in \mathbb{R}_{\geq 0}^J \mid \sum_{j=1}^J \lambda_j = 1 \right\}, \quad (14)$$

where  $\lambda^*$  solves the dual quadratic program

$$\min_{\lambda \in \Delta_J} \frac{1}{2} \lambda^\top G_m G_m^\top \lambda - \lambda^\top f(\theta_m). \quad (15)$$

Hence  $\delta_m^*$  is a linear combination of all subgroup gradients at iteration  $m$ .

The proof of Theorem 1 following previous work (Shen et al. 2022) is given in Appendix A. This theorem indicates that the original constrained min-max problem can be reformulated as a dual quadratic programming problem with dimensionality  $J$  (the number of noise subgroups). Instead of optimizing high-dimensional vectors, the solution now consists of a linear combination of subgroup gradients. This reformulation reduces the computational cost to  $O(J^3)$ . Statistically, the convex combination coefficients serve as a weight vector assigning importance across subgroups. Theorem 1 proves that DRIQN can enhance data utilization compared to methods relying solely on worst-case scenarios.

For the convergence of DRIQN, the model training is based on the stochastic approximation of the gradient. Due to the boundedness of the mini-batch gradients of the objective function  $\max_{1 \leq j \leq J} f_j(\theta_m) + \langle \nabla f_j(\theta_m), \theta - \theta_m \rangle$ , the stochastic convergence rate is  $\mathcal{O}(T^{-1/2})$  following the conclusion in (Hazan, Agarwal, and Kale 2006), where  $T$  denotes the iteration times.

## Experiments

### Experimental Settings

**Simulation Environment.** To bring the simulation closer to real sea-surface conditions characterized by uncertain haz-

ards such as inconspicuous current vortices and reef obstacles, we employ a risky marine environment under perturbation based on previous work (Lin, McConnell, and Englot 2023) and deploy a purely sensor-based navigation scheme without any prior knowledge. Given our focus on robust policy optimization under severe observational noise, the environment features 4 vortices and 6 obstacles randomly dispersed across the operational space. To mitigate randomness, we train the models for a total of 1.5 million time steps across nine different random seeds. During the evaluation stage, the positions of both the goal and start point are reset each time, allowing exploration of different environmental conditions and capturing the varying noise patterns. Agents undergo evaluation every 10,000 training steps across 15 pre-randomized environments.

**Noise Settings.** To enhance the perception robustness of IQN agent for our purposes, we implement the DRIQN based on this environment and posit that the critical challenge lies in maintaining the robustness of DistRL under noisy observation. In order to narrow the gap between simulation and real sea-surface sensing, we ground our noise modeling in prior physical studies (Koenig and Howard 2004; Laconte et al. 2021) and superimpose ubiquitous non-synthetic sensor noise processes, specifically Gaussian and Poisson noise. To assess DRIQN’s multi-noise robustness, *The Analysis of “Noise-Type”* incorporates extra salt-and-pepper noise (simulating extreme value fluctuations) and occlusion noise (emulating partial sensor failures). This DRO framework is agnostic to the specific noise law, enabling extensions to other settings, including safety analysis under adversarial perturbations. The noise intensity is configured as a tunable hyperparameter, with values empirically set to  $\{0.6, 0.4, 0.2\}$  to evaluate performance degradation across perturbation levels systematically. The sensor value range and noise intensity both determine the distributions.

**Baselines.** We compare DRIQN with the following representative methods in USV navigation: (1) Classical observation-based planning methods: Artificial Potential Field (APF) method (Fan et al. 2020) and Bug Algorithm (BA) method (Lumelsky and Skewis 1988); (2) Standard Q-learning method in DRL: DQN (Mnih et al. 2015); (3) Risk-sensitive method in DistRL: IQN (Dabney et al. 2018).

**Hyperparameter Settings.** For neural networks with three or more layers, we implement gradient substitution exclusively in the final layer instead of the whole layers, inspired by established computer vision research on gradient manipulation (Shen et al. 2022). The comparative analysis is detailed in Section: *The Analysis of “Gradient Substitution”*. Additionally, to adapt the gradients computed by the DRO to the training of all layers except the final one, we adapt the learning rate decay of these layers starting from 0.0001 to 0.000001 and appropriately shrink the calculated gradients. The experiments were completed in parallel using six A6000 GPUs and AMD EPYC 7542 CPU.

### Metrics and Strategy

**Metrics.** To evaluate the performance of our approach, we employed six metrics encompassing performance, safety, and efficiency: success rate (SR), collision rate (CR), time-



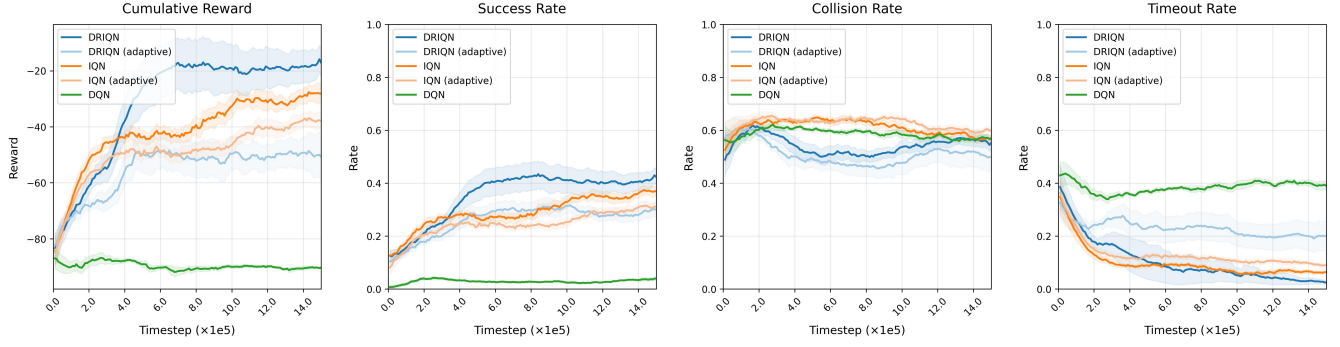


Figure 3: Online evaluations compare three learning-based models and two distributional RL strategies. Performance, safety, and convergence are assessed via three key metrics with cumulative reward curves. Implementation details appear in *Experimental Settings*. Due to space limit, the other two figures beyond noise level 0.6 are in Appendix B.

Method	Strategy	Success Rate $\uparrow$			Collision Rate $\downarrow$			Timeout Rate $\downarrow$			Final Reward $\uparrow$			Avg Time $\downarrow$			Avg Energy $\downarrow$		
		0.6	0.4	0.2	0.6	0.4	0.2	0.6	0.4	0.2	0.6	0.4	0.2	0.6	0.4	0.2	0.6	0.4	0.2
APF	—	0.11	0.25	0.03	0.81	0.55	0.53	0.08	<u>0.20</u>	0.44	—	—	—	206.68	349.32	547.89	320.96	654.48	1071.70
BA	—	0.22	0.11	0.26	0.71	0.46	<b>0.33</b>	0.07	0.43	0.41	—	—	—	185.76	482.98	462.97	251.11	691.93	691.57
DQN	Greedy	0.04	0.03	0.02	<u>0.57</u>	0.57	0.57	0.39	0.40	0.41	-90.30	-90.11	-89.54	541.27	550.35	560.52	858.39	779.78	832.67
IQN	Greedy	<u>0.37</u>	<u>0.50</u>	<u>0.61</u>	<u>0.57</u>	<u>0.45</u>	<u>0.37</u>	<u>0.06</u>	<b>0.04</b>	0.02	-28.16	-14.87	13.47	144.89	123.75	61.25	196.73	181.63	92.18
	Adaptive	0.31	0.36	0.46	0.60	0.51	0.38	0.09	0.13	0.16	-37.93	-38.97	-48.66	185.75	230.00	274.27	247.34	296.00	358.99
DRIQN	Greedy	<b>0.42</b>	<b>0.55</b>	<b>0.63</b>	0.55	<b>0.42</b>	<u>0.37</u>	<b>0.02</b>	<b>0.04</b>	<b>0.01</b>	-17.11	<b>3.14</b>	<b>26.87</b>	<b>93.51</b>	<b>90.11</b>	<b>31.82</b>	<b>141.67</b>	<b>114.15</b>	<b>53.61</b>
	Adaptive	0.30	0.39	0.33	<b>0.50</b>	0.46	0.49	0.20	0.15	0.18	-50.84	-36.16	-45.90	283.85	226.07	272.25	392.90	257.17	401.26
Improvement (%)		<b>13.51</b>	<b>10.00</b>	<b>3.28</b>	<b>12.28</b>	<b>6.67</b>	-12.12	<b>66.67</b>	—	<b>50.00</b>	<b>39.24</b>	<b>121.12</b>	<b>99.48</b>	<b>35.46</b>	<b>27.18</b>	<b>48.05</b>	<b>27.99</b>	<b>37.15</b>	<b>41.84</b>

Table 1: **Overall performance comparison** under three different noise levels (0.6, 0.4, and 0.2) related to the variances of the noise distributions. The best results are highlighted in **bold** and the second best results are highlighted with an underline. “Improvement” denotes the percentage increase (positive metrics) or decrease (negative metrics) over the second best models.

out rate (TR), final (cumulative) reward (FCR), average time consumed (AT), and average energy consumed (AE). Average time and energy are calculated based solely on data from successful episodes.

**Strategy.** We compare the standard greedy strategy, which always selects the action with the highest expected reward, with an adaptive strategy for the IQN-based methods proposed by (Lin, McConnell, and Englot 2023). The adaptive strategy adaptively tailors the region of interest in return distributions through computing CVaR threshold based on real-time environmental risk assessments. This threshold reflects different levels of risk sensitivity, measured by the robot’s distance to the nearest obstacles. When no obstacles are detected, the adaptive strategy behaves like a greedy one.

## Performance Comparison

Online evaluation results displayed in Figure 3 are smoothed by Exponential Moving Average to describe learning curves with shaded regions showing standard deviations over 9 seeds under high noise variance (level=0.6).

Key performance illustrated in Table 1 are further summarized as follows:

- **DRIQN vs. Baseline Methods:** As a DistRL approach

enhanced by DRO-based gradient substitution, DRIQN achieves superior success / collision rates and impressive efficiency compared with other traditional physical methods and RL algorithms across noise intensities, particularly under high noise variance.

- **DistRL vs. Standard RL:** DistRL methods consistently outperform standard deep Q-learning. DQN suffers from high timeout rates and excessive resource consumption due to passive collision avoidance behaviors, a limitation rooted in standard RL’s dependence on expected returns that provide inadequate information in noisy environments. In contrast, DistRL’s explicit modeling of return distributions yields inherent noise robustness.
- **Greedy vs. Adaptive:** Both IQN and DRIQN show higher success rates with greedy action selection. Adaptive strategies suffer under noise interference as perturbed value distributions impair their decision mechanism.
- **DRIQN Efficiency:** Under stringent noise-corrupted conditions, greedy DRIQN maintains the lowest timeout rate while reducing energy and time consumption, optimally balancing safety and efficiency.

The qualitative trajectory results of RL agents are visualized in Figure 4.

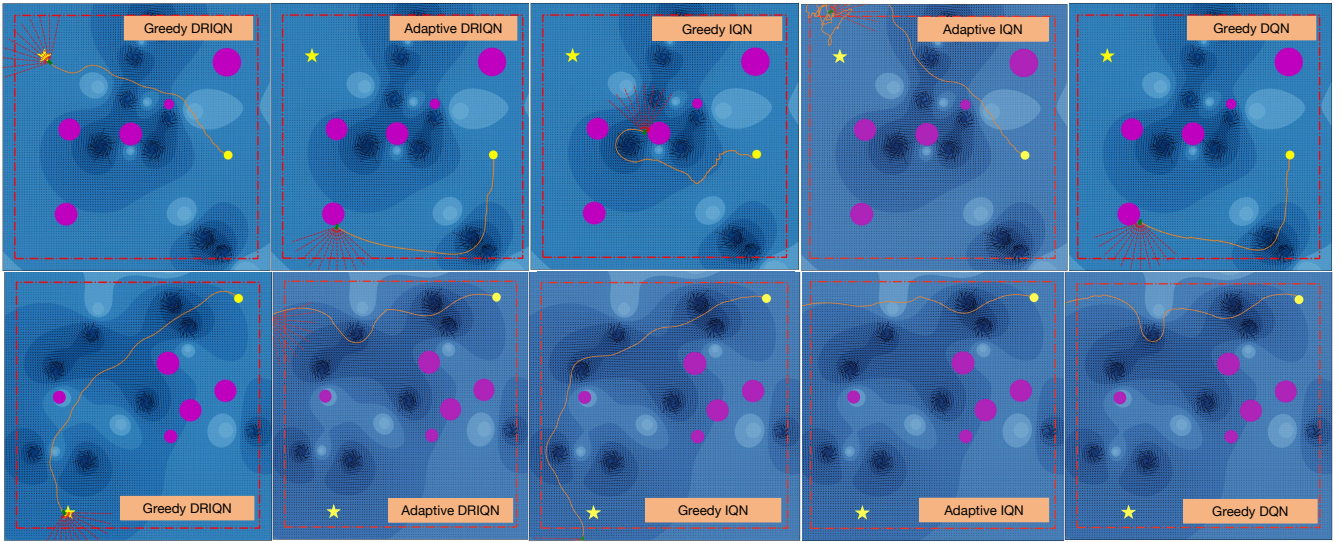


Figure 4: **Qualitative trajectory results** (noise variance level = 0.6). The greedy approach avoids risk-sensitive adjustments triggered by noisy observations, unlike the adaptive strategy. Aligning with Table 1, the adaptive strategy exhibits higher timeout rates and frequent deviations from complex conditions to mitigate risk, as seen in repeated trials.

Model	SR $\uparrow$	CR $\downarrow$	TR $\downarrow$	FCR $\uparrow$	AT $\downarrow$	AE $\downarrow$
APF	0.12	0.80	0.08	—	211.83	351.38
BA	0.14	0.82	0.04	—	134.65	198.20
DQN	0.11	0.50	0.39	-80.02	507.04	798.70
IQN	0.54	0.44	0.02	-3.32	75.27	108.54
DRIQN	<b>0.58</b>	<b>0.41</b>	<b>0.01</b>	<b>12.45</b>	<b>45.10</b>	<b>73.30</b>

Table 2: Comparison of multi-noise robustness performance, with the best method highlighted in **bold**.

### The Analysis of “Noise Types”

To rigorously evaluate DRIQN’s safety in multi-noise conditions, we augment natural noise conditions with salt-and-pepper noise (simulating sensor malfunction) and occlusion noise (emulating data loss scenarios) for faulty sensors, setting a fractionally lower noise intensity across all sufficient perturbations for intensity-diversity balance. The strategy is rigged to greedy rather than adaptive for more competitive performance in this task, as empirically demonstrated earlier. Evidenced in Table 2, DRIQN’s optimization across heterogeneous noise subgroups demonstrates superior handling of complex perceptual patterns and observational robustness over baselines.

### The Analysis of “Gradient Substitution”

To examine our last-layer gradient substitution setting for DRIQN, we introduce the variant DRIQN-W featuring whole-network (4-layer) gradient replacement for comparison. As evidenced in Table 3, last-layer substitution significantly outperforms whole-network gradient replacement in both success rate and computational efficiency while ensuring better safety. This advantage stems from its capacity to retain deep neural networks’ representational benefits

Model	Strategy	SR $\uparrow$	CR $\downarrow$	AT $\downarrow$
DRIQN	Greedy	<b>0.42</b>	0.55	<b>93.51</b>
	Adaptive	0.30	<b>0.50</b>	283.85
DRIQN-W	Greedy	<u>0.22</u>	<u>0.54</u>	<u>357.87</u>
	Adaptive	0.20	0.55	379.50

Table 3: Architectural comparison of “gradient substitution” under high noise variance: Whole-network substitution (DRIQN-W) versus final-layer substitution (DRIQN).

while enhancing robustness through streamlined optimization, even under extreme noise conditions. Learning curves comparison in Appendix C shows that last-layer substitution has better convergence than full-network modification.

## Conclusion

In this paper, we introduce DRIQN, a robust and efficient distributional RL policy for USV path planning in unknown marine environments subject to observation noise. DRIQN addresses limitations of vanilla DistRL with implicit quantile networks in robustness and efficiency by employing a flexible gradient substitution method that uses DRO for gradient calculation, enabling the policy to handle complex observation noise patterns. Experimental results confirm DRIQN’s superiority across all six metrics in performance, safety, and efficiency domains, outperforming SOTA methods. Results also reveal that within DistRL, the greedy strategy outperforms adaptive counterpart under noisy observational conditions. In future work, we plan to explore additional DistRL methods to enhance robustness and broaden our approach to more diverse environmental settings. We also aim to validate effectiveness of these methods in real-world deployments, ensuring practical applicability.

## References

- Asfihani, T.; Maulana Syafi'i, A.; and Hasan, A. 2025. Fault-tolerant model predictive control for unmanned surface vehicles. *Systems Science & Control Engineering*, 13(1): 2469598.
- Dabney, W.; Ostrovski, G.; Silver, D.; and Munos, R. 2018. Implicit quantile networks for distributional reinforcement learning. In *International conference on machine learning*, 1096–1105. PMLR.
- Dawood, M.; Shokry, A.; and Bennewitz, M. 2024. A Dynamic Safety Shield for Safe and Efficient Reinforcement Learning of Navigation Tasks. *ArXiv*, abs/2412.04153.
- Elmakis, O.; and Degani, A. 2023. USV port oil spill cleanup using hybrid multi-destination RL-CPP. *IEEE Access*, 11: 122722–122735.
- Fan, X.; Guo, Y.; Liu, H.; Wei, B.; and Lyu, W. 2020. Improved Artificial Potential Field Method Applied for AUV Path Planning. *Mathematical Problems in Engineering*.
- Fernandes, J. F.; Assunção, M.; Serrano, D.; Afonso, P.; Pinheiro, P.; Marques, H.; Neves, J.; Teodoro, P.; Póvoa, R.; Marat-Mendes, R.; et al. 2025. A smart energy management system for surface unmanned vehicles for border surveillance missions. *Scientific Reports*, 15(1): 23684.
- Han, J.; Park, J.; Kim, J.; and Son, N.-s. 2016. GPS-less coastal navigation using marine radar for USV operation. *Ifac-papersonline*, 49(23): 598–603.
- Hazan, E.; Agarwal, A.; and Kale, S. 2006. Logarithmic regret algorithms for online convex optimization. *Machine Learning*, 69: 169–192.
- He, Y.; Liu, Z.; Wang, W.; and Xu, P. 2025. Sample Complexity of Distributionally Robust Off-Dynamics Reinforcement Learning with Online Interaction. In *Forty-second International Conference on Machine Learning*.
- Hong, L.; Liu, H.; Yang, Q.; and Yao, J. 2024. Model predictive attitude control of unmanned surface vehicle based on short-time wave prediction. *Ocean Engineering*, 314: 119727.
- Hossain, J.; Faridee, A.-Z.; Asher, D.; Freeman, J.; Trout, T.; Gregory, T.; and Roy, N. 2024. QuasiNav: Asymmetric Cost-Aware Navigation Planning with Constrained Quasimetric Reinforcement Learning. *arXiv preprint arXiv:2410.16666*.
- Huber, P. J. 1992. Robust estimation of a location parameter. In *Breakthroughs in statistics: Methodology and distribution*, 492–518. Springer.
- Khatib, O. 1985. Real-Time Obstacle Avoidance for Manipulators and Mobile Robots. *The International Journal of Robotics Research*, 5: 90 – 98.
- Koenig, N.; and Howard, A. 2004. Design and Use Paradigms for Gazebo, An Open-Source Multi-Robot Simulator. In *Proceedings of the IEEE/RSJ International Conference on Intelligent Robots and Systems (IROS)*, 2149–2154.
- Laconte, J.; Randriamiarintsoa, E.; Kasmi, A.; Pomerleau, F.; Chapuis, R.; Debain, C.; and Aufrère, R. 2021. Dynamic Lambda-Field: A Counterpart of the Bayesian Occupancy Grid for Risk Assessment in Dynamic Environments. 2021 *IEEE/RSJ International Conference on Intelligent Robots and Systems (IROS)*, 4846–4853.
- Lee, K.; Kim, S.; and Choi, J. 2023. Adaptive and explainable deployment of navigation skills via hierarchical deep reinforcement learning. In *2023 IEEE International Conference on Robotics and Automation (ICRA)*, 1673–1679. IEEE.
- Leung, C. H.; Huang, Y.; Li, Y.; and Wu, Q. 2025. Distributionally Robust Policy Evaluation and Learning for Continuous Treatment with Observational Data. *ArXiv*, abs/2501.10693.
- Lin, X.; McConnell, J.; and Englot, B. 2023. Robust unmanned surface vehicle navigation with distributional reinforcement learning. In *2023 IEEE/RSJ International Conference on Intelligent Robots and Systems (IROS)*, 6185–6191. IEEE.
- Liu, C.; van Kampen, E.-J.; and De Croon, G. C. 2023. Adaptive risk-tendency: Nano drone navigation in cluttered environments with distributional reinforcement learning. In *2023 IEEE International Conference on Robotics and Automation (ICRA)*, 7198–7204. IEEE.
- Lolla, T.; Haley Jr, P. J.; and Lermusiaux, P. F. 2015. Path planning in multi-scale ocean flows: Coordination and dynamic obstacles. *Ocean Modelling*, 94: 46–66.
- Lumelsky, V. J.; and Skewis, T. 1988. A paradigm for incorporating vision in the robot navigation function. *Proceedings. 1988 IEEE International Conference on Robotics and Automation*, 734–739 vol.2.
- Lumelsky, V. J.; and Stepanov, A. A. 1986. Dynamic path planning for a mobile automaton with limited information on the environment. *IEEE Transactions on Automatic Control*, 31: 1058–1063.
- Lütjens, B.; Everett, M.; and How, J. P. 2018. Safe Reinforcement Learning With Model Uncertainty Estimates. *2019 International Conference on Robotics and Automation (ICRA)*, 8662–8668.
- McGuire, K. N.; de Croon, G. C.; and Tuyls, K. 2018. A Comparative Study of Bug Algorithms for Robot Navigation. *Robotics Auton. Syst.*, 121.
- Menges, D.; Tengesdal, T.; and Rasheed, A. 2024. Non-linear model predictive control for enhanced navigation of autonomous surface vessels. *IFAC-PapersOnLine*, 58(18): 296–302.
- Mnih, V.; Kavukcuoglu, K.; Silver, D.; Rusu, A. A.; Veness, J.; Bellemare, M. G.; Graves, A.; Riedmiller, M. A.; Fidjeland, A. K.; Ostrovski, G.; Petersen, S.; Beattie, C.; Sadik, A.; Antonoglou, I.; King, H.; Kumaran, D.; Wierstra, D.; Legg, S.; and Hassabis, D. 2015. Human-level control through deep reinforcement learning. *Nature*, 518: 529–533.
- Nietert, S.; Goldfeld, Z.; and Shafiee, S. 2023. Outlier-robust wasserstein dro. *Advances in Neural Information Processing Systems*, 36: 62792–62820.
- Qi, Q.; Guo, Z.; Xu, Y.; Jin, R.; and Yang, T. 2020. An Online Method for A Class of Distributionally Robust Optimization with Non-convex Objectives. In *Neural Information Processing Systems*.



- Ramesh, S. S.; Sessa, P. G.; Hu, Y.; Krause, A.; and Bogunovic, I. 2024. Distributionally robust model-based reinforcement learning with large state spaces. In *International Conference on Artificial Intelligence and Statistics*, 100–108. PMLR.
- Shen, X.; Wang, X.; Xu, Q.; Ge, W.; and Xue, X. 2022. Towards Scalable and Fast Distributionally Robust Optimization for Data-Driven Deep Learning. In *2022 IEEE International Conference on Data Mining (ICDM)*, 448–457. IEEE.
- Shi, J.; Bai, C.; He, H.; Han, L.; Wang, D.; Zhao, B.; Zhao, M.; Li, X.; and Li, X. 2024a. Robust quadrupedal locomotion via risk-averse policy learning. In *2024 IEEE International Conference on Robotics and Automation (ICRA)*, 11459–11466. IEEE.
- Shi, L.; and Chi, Y. 2024. Distributionally robust model-based offline reinforcement learning with near-optimal sample complexity. *Journal of Machine Learning Research*, 25(200): 1–91.
- Shi, L.; Li, G.; Wei, Y.; Chen, Y.; Geist, M.; and Chi, Y. 2024b. The curious price of distributional robustness in reinforcement learning with a generative model. *Advances in Neural Information Processing Systems*, 36.
- Staib, M.; and Jegelka, S. 2019. Distributionally robust optimization and generalization in kernel methods. *Advances in Neural Information Processing Systems*, 32.
- Sun, J.; Liu, G.; Tian, G.; and Zhang, J. 2019. Smart Obstacle Avoidance Using a Danger Index for a Dynamic Environment. *Applied Sciences*.
- Tobin, J.; Fong, R.; Ray, A.; Schneider, J.; Zaremba, W.; and Abbeel, P. 2017. Domain randomization for transferring deep neural networks from simulation to the real world. *2017 IEEE/RSJ International Conference on Intelligent Robots and Systems (IROS)*, 23–30.
- Tomilin, T.; Fang, M.; and Pechenizkiy, M. 2025. HASARD: A Benchmark for Vision-Based Safe Reinforcement Learning in Embodied Agents. In *The Thirteenth International Conference on Learning Representations*.
- Tran, H. D.; Nguyen, N. T.; Cao, T. N. T.; Gia, L. X.; Ho, K.; Nguyen, D. D.; Pham, B. T.; and Truong, V. N. 2024. Unmanned surface vehicle for automatic water quality monitoring. In *E3S Web of Conferences*, volume 496, 03005. EDP Sciences.
- Vieira, M.; Amorim, M. C. P.; Sundelöf, A.; Prista, N.; and Fonseca, P. J. 2020. Underwater noise recognition of marine vessels passages: Two case studies using hidden Markov models. *ICES Journal of Marine Science*, 77(6): 2157–2170.
- Wang, J.; Xia, L.; Peng, L.; Li, H.; and Cui, Y. 2023a. Efficient uncertainty propagation in model-based reinforcement learning unmanned surface vehicle using unscented kalman filter. *Drones*, 7(4): 228.
- Wang, N.; Wang, Y.; Zhao, Y.; Wang, Y.; and Li, Z. 2022. Sim-to-real: Mapless navigation for USVs using deep reinforcement learning. *Journal of Marine Science and Engineering*, 10(7): 895.
- Wang, Y.; Liu, W.; Liu, J.; and Sun, C. 2023b. Cooperative USV-UAV marine search and rescue with visual navigation and reinforcement learning-based control. *ISA transactions*, 137: 222–235.
- Zhang, H.; Zhao, G.; and Ren, X. 2025. TERL: Large-Scale Multi-Target Encirclement Using Transformer-Enhanced Reinforcement Learning. *arXiv preprint arXiv:2503.12395*.